

Theoretical Study of Novel Porphyrins Bearing Electron Donor–Acceptor Groups

Carolina Caicedo, Ana Martínez* and Ernesto Rivera

This research project is focused on molecules that comprise a series of asymmetrically A₃B-type meso-substituted free-base porphyrins and their related Zn-metalloporphyrins. A and B were taken as electron-donor and electron-acceptor groups. Full geometry optimizations without symmetry constraints were performed with B3LYP/6-31G(d,P) methodology. Time-dependent density functional theory calculations of the optimized structures indicate that there is a good agreement with the available experimental results. The highest occupied molecular orbital–lowest occupied molecular orbital (LUMO) gaps (ranging between 2.62 and 2.80 eV) are similar to those reported before for other porphyrins (2.29 eV). Also, the LUMO

is situated close to the conduction band of titanium oxide, increasing the possibility of a charge transfer process. As porphyrins may act as electron transfer systems, the electron donor–acceptor capacity of these systems is characterized using two parameters; electrodonating (χ^-) and electroaccepting (χ^+) electronegativity. The main goal of this investigation is to analyze the electronic structure and the donor–acceptor properties of these porphyrins to see if these compounds could be useful for further applications related to the design of solar cells. © 2012 Wiley Periodicals, Inc.

DOI: 10.1002/qua.24316

Introduction

Porphyrins are part of a very important family of fluorophores, which have been widely studied in the context of macromolecular and material sciences.^[1–4] These chromophores are highly delocalized π -systems, considered as a unique category of ionic scavengers, whose defined characteristics arise from the heteroatoms present in their structure.^[5] Because of their efficient light absorption, porphyrins have been the subject of intense research for the purpose of solar energy transfer and electron transfer systems.^[6–9] The incorporation of porphyrins into polymers permits easy handling, recycling, and adaptation of this important set of complexant agents for ongoing processes. Porphyrins have also been used in the synthesis of push-pull π -conjugated systems bearing electron-donor and electron-acceptor groups and also in the design of dendritic molecules able to act as molecular antennae for photovoltaic applications.^[6,7] Moreover, several electro- and photoactive units have been incorporated into porphyrins to tune their electronic and photophysical properties. The electron donor–acceptor character of porphyrins can also be modified, depending on their coordination state and their photoactive units which are linked together.^[10–12] Thus, the preparation, electronic, and optical properties of several porphyrin derivatives, linked to electro- and photoactive units such as fullerene C₆₀,^[10] anthracene,^[11] pyrene,^[12] and functionalized porphyrins^[13] have been described in the literature. In the context of theoretical studies, certain authors use density functional theory (DFT) calculations,^[14–24] to study the geometry and electronic structure of porphyrins with varying substituents for the purpose of designing an efficient material with the potential applications of an organic-based dye for solar cells. Usually, the absorption spectra are interpreted qualitatively in terms of the Gouterman's four-orbital model^[25–27] which only considers

transition in the cases of the two highest occupied and the two lowest unoccupied molecular orbitals.

In previous works, it has been established that the porphyrin synthesizers for dye-sensitized solar cells must absorb most of the radiation from the solar light in the near-IR and visible regions and for this purpose, the energy difference between the highest occupied molecular orbital (HOMO) and the lowest occupied molecular orbital (LUMO) should be approximately 2 eV, since this value corresponds to the maximum in the solar radiation energy spectrum. For this reason, the HOMO–LUMO energy gap is a good parameter to analyze the potential efficiency of these materials. Likewise, it is important that the LUMO to be situated above and close to the conduction band of titanium oxide, to augment the charge transfer character. Using these two parameters: the HOMO–LUMO gap and the value of the LUMO energy when compared to the conduction band of titanium oxide, in a previous work,^[17] the authors analyzed Zn meso-tetraphenylporphyrin (ZnTPP) complexes bearing different substituents and found that inserting thiophene units produces materials that improve these properties than porphyrins with other substituents. Another report^[18] indicated that the asymmetric substitution of the porphyrin rings will result in a strong mixing of configurations, which contributes to the red shift of the absorption spectra. In all these studies, the absorption spectra were analyzed with reference to Gouterman's four orbital model.

C. Caicedo, A. Martínez, E. Rivera
Instituto de Investigaciones en Materiales, Universidad Nacional Autónoma de México. Ciudad Universitaria, C.P. 04510 México D.F. México
E-mail: martina@iim.unam.mx

© 2012 Wiley Periodicals, Inc.

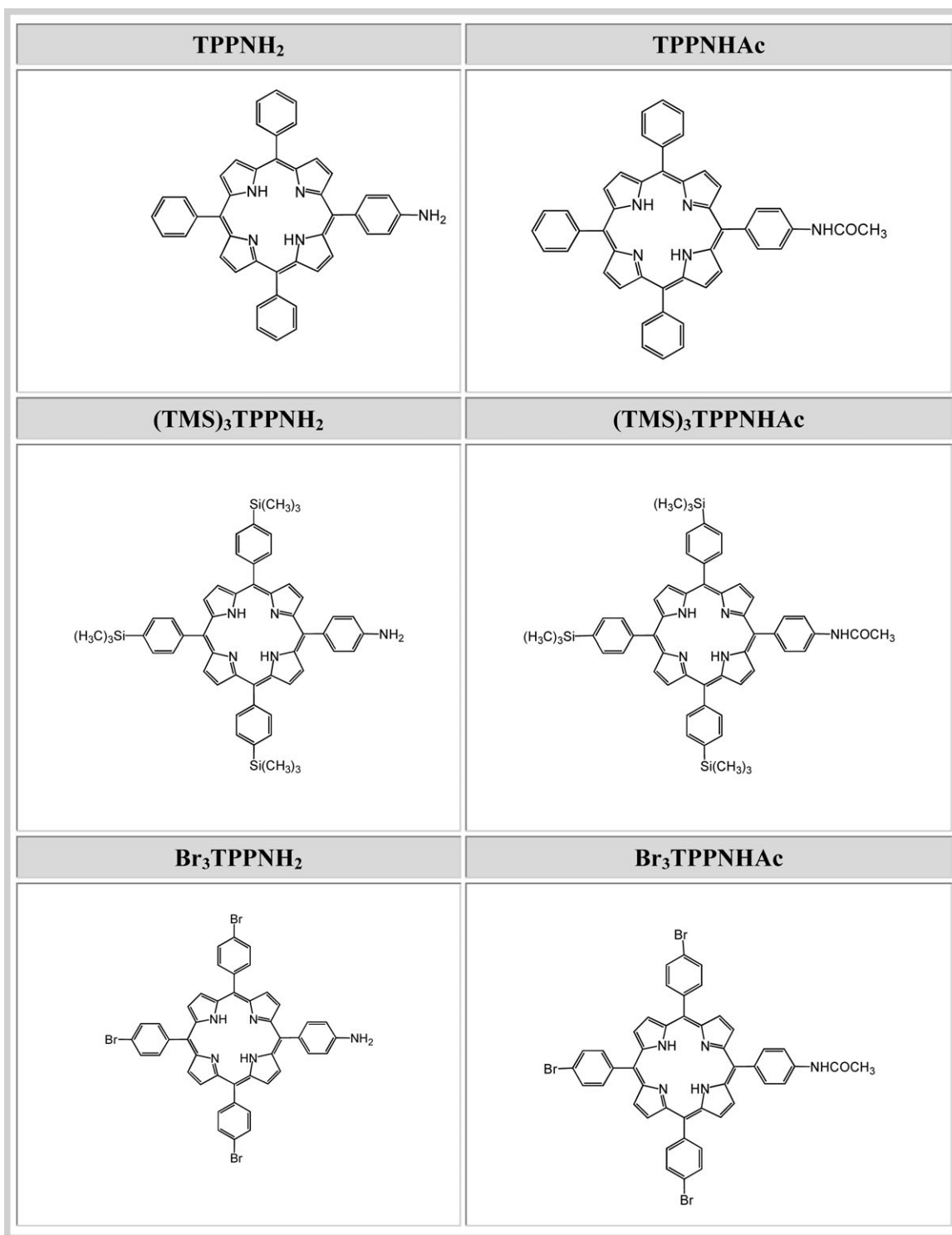


Figure 1. Molecular structures of the studied compounds. The corresponding Zn metallated were also analyzed.

In view of the fact that the design of molecular antennae and push-pull π -conjugated systems is one of the main interests of our group, we performed the synthesis and characterization of some porphyrin derivatives that are unusual in terms of their solubility in common organic solvents and their capacity of acting either as electron-donor or electron-acceptor groups (see Supporting Information). The meso-substituted free-base porphyrins that were synthesized are:

5-(4-aminophenyl)10,15,20-triphenyl porphyrin (TPPNH₂) and 5-(4-acetamidophenyl) 10,15,20-triphenyl porphyrin (TPPNHAc) with different substituents as illustrated in Figure 1. These constitute meso-substituted A₃B-type porphyrins which contain two different groups that are electron-donors: aminophenyl and acetamidophenyl. Another substituent is bromide (Br) which is a very well-known electron-acceptor. Trimethylsilyl (TMS) was also used to find a substituent that is neither an

electron donor nor an electron acceptor group. The optical properties of all these compounds have been determined by absorption spectroscopy (experimental details are included as Supporting Information). It is important to note that neither the synthesis, nor the electronic structure of TPPNH₂ and TPPNHAc porphyrins has previously been reported. The theoretical study of the related Zn-metalloporphyrins is also discussed. Time-dependent DFT (TD-DFT) calculations have been carried out with B3LYP, to make a comparison between the theoretical and the experimental UV–visible spectra. This methodology was previously used with success in the study of other molecules and porphyrins.^[16,17,20–24] The electronic structure of these porphyrins was also determined to find materials that are apt for creating solar cells. To facilitate the charge transfer to the electrodes in a solar cell, it is important to have an electron-donor group with low ionization energy and an electron-acceptor group with high electron affinity. Considering that porphyrins may act as electron transfer systems, it is worth to characterize the electron donor–acceptor capacity of these systems. In this report, we propose two parameters; electrodonating (χ^-) and electroaccepting (χ^+) electronegativity, to characterize these compounds. Thus, the main goal of this investigation is to analyze the electronic structure and the donor–acceptor properties of these porphyrins.

Computational Details

Previous TD-DFT benchmark^[28] reports indicate that the results obtained with B3LYP are in good agreement with experimental values. Density functional approximation^[29] as implemented in *Gaussian 09*^[31] was used for all calculations. Full geometry optimization without symmetry constraints and frequency analyses were carried out for all the stationary points using the three parameters hybrid B3LYP functional.^[32] In all cases, calculations were done in gas phase with 6-31g (d,p) basis sets.^[33] Harmonic frequency analysis allowed us to verify optimized minima. The local minima were identified with the number of imaginary frequencies (NIMAG = 0). The absorption spectra have been computed with TD-DFT using B3LYP functional and the same basis sets. Theoretically, the intensity of the band is expressed in terms of the oscillator strengths (f). Stationary points were first modeled in gas phase (vacuum), and solvent effects were included *a posteriori*, applying single point calculations at the same level of theory, using a polarisable continuum model, specifically the integral-equation-formalism-PCM (Polarisable Continuum

Model)^[34,35] with chloroform as solvent to make a comparison with available experimental results.

In DFT, the first derivative of the energy with respect to the number of electrons at constant external potential is identified as the chemical potential, μ . From the results of Gázquez et al.^[36] it is possible to define two different electronegativities for the charge transfer process: one that describes the donation (χ^-) and another one that is useful for the electron acceptance (χ^+).

$$\chi^- = \frac{1}{4}(3I + A) \quad (1)$$

$$\chi^+ = \frac{1}{4}(I + 3A) \quad (2)$$

Lower values of χ^- imply a better electron donor and larger values of χ^+ represent a better electron acceptor character. These parameters were used with success previously.^[37] I and A refer to one electron transfer processes whilst χ^- and χ^+ consider fractional charge transfer reactions. As the partial charge transfer is one of the main intermolecular factors that dominates the binding energies in many reactions, χ^- and χ^+ will be better parameters than I and A to describe the electron donor–acceptor properties of these systems.

Results and Discussion

UV–visible spectra

In Table 1, we present the obtained results for the six substituted TPPNH₂ and TPPNHAc porphyrins shown in Figure 1 and

Table 1. Theoretical and available experimental data (see Supporting Information) of the maximum absorption UV–vis.

Label	λ_{max} (nm) Theo	λ_{max} (nm) Exp	MO	Energy (eV)	f	Electronic transition configurations
TPPNH ₂	393	419	L+1	-2.12	1.42	H-1 → L (35%)
			L	-2.14		H-2 → L+1 (23%)
			H	-4.78		H → L+1 (23%)
			H-1	-5.14		H → L+1 (19%)
(TMS) ₃ TPPNH ₂	395	422	L+1	-2.11	1.49	H-1 → L (35%)
			L	-2.13		H-2 → L+1 (23%)
			H	-4.76		H → L+1 (22%)
			H-1	-5.13		H-1 → L+1 (20%)
Br ₃ TPPNH ₂	396	422	L+1	-2.38	1.55	H-1 → L (34%)
			L	-2.41		H-1 → L+1 (25%)
			H	-5.03		H → L+1 (21%)
			H-1	-5.40		H-2 → L+1 (20%)
TPPNHAc	402	419	L+1	-2.30	1.68	H-1 → L (45%)
			L	-2.32		H → L+1 (30%)
			H	-4.98		H-1 → L+1 (15%)
			H-1	-5.31		H → L (10%)
(TMS) ₃ TPPNHAc	404	421	L+1	-2.28	1.86	H-1 → L (38%)
			L	-2.30		H → L+1 (26%)
			H	-4.96		H-1 → L+1 (22%)
			H-1	-5.29		H → L (14%)
Br ₃ TPPNHAc	406	422	L+1	-2.56	z	H-1 → L+1 (39%)
			L	-2.58		H → L (25%)
			H	-5.23		H-1 → L (21%)
			H-1	-5.57		H → L+1 (15%)

Molecular orbital contribution of the two HUMO and two LUMO of TPPNH₂ and TPPNHAc porphyrins, oscillator strength (f), and electronic transition configuration composition.

Table 2. Theoretical data of the maximum absorption UV-vis

Label	λ_{\max} (nm)	MO	Energy (eV)	f	Electronic transition configurations
TPPNH ₂ -Zn	398	L+1	-2.05	0.95	H-1 → L+1 (30%) H-2 → L (27%) H-3 → L (24%) H → L (19%)
		L	-2.06		
		H	-4.84		
(TMS) ₃ TPPNH ₂ -Zn	400	L+1	-2.04	1.13	H-1 → L+1 (32%) H-2 → L (29%) H-3 → L (21%) H → L (18%)
		L	-2.06		
		H	-4.82		
Br ₃ TPPNH ₂ -Zn	402	L+1	-2.31	1.20	H-1 → L+1 (33%) H-2 → L (25%) H-3 → L (22%) H → L (20%)
		L	-2.34		
		H	-5.08		
TPPNHAc-Zn	406	L+1	-2.23	1.56	H-1 → L+1 (47%) H → L (34%) H-3 → L (19%) -
		L	-2.24		
		H	-5.04		
(TMS) ₃ TPPNHAc-Zn	407	L+1	-2.21	1.65	H-1 → L+1 (48%) H → L (35%) H-3 → L (17%) -
		L	-2.22		
		H	-5.02		
Br ₃ TPPNHAc-Zn	409	L+1	-2.49	1.64	H-1 → L (43%) H → L+1 (32%) H-3 → L+1 (14%) H-2 → L+1 (11%)
		L	-2.50		
		H	-5.29		
		H-1	-5.50		

Molecular orbital contribution of the two HOMO and two LUMO of Zn-metalloporphyrins, oscillator strength (f), and electronic transition configuration composition.

those of their corresponding Zn-metallated porphyrins are summarized in Table 2. There are no experimental results for the last ones, but it is possible to use the theoretical values to anticipate the influence of the metal on the UV-visible spectra. In metallated porphyrins, the porphyrin ring system is completely deprotonated. In fact, the metal ion is an acid of Lewis, whereas the deprotonated porphyrins are dianionic ligands and act as Lewis bases; this means that the metal will accept lone pairs of electrons from the porphyrins.

TPPNH₂ and TPPNHAc porphyrins have asymmetric substituted rings so that we can observe a strong mixing of configurations. All the compounds shown in Table 1 exhibited an experimental λ_{\max} value in the range of 419–422 nm, whereas theoretical values fall between 393 and 406 nm, thereby indicating that the maximum error is 6.1%. The bands of TPPNH₂ and TPPNHAc bearing acceptor groups such as Br are slightly red-shifted with respect to the nonsubstituted porphyrins (TPPNHAc vs. Br₃TPPNHAc, for example), which is in agreement with the experimental results.

The comparison of the calculated λ_{\max} of TPPNH₂ and TPPNHAc porphyrins (Table 1) and the corresponding Zn-metalloporphyrins (Table 2) indicates that in all cases there is a bathochromic shift of the maxima absorption bands due to the presence of this metal. This means that a decrement occurs in terms of the π to π^* energy gap. It is important to remember that metallated porphyrins with Zn are so-called regular metalloporphyrins because they present closed-shell metal atoms. The $d\pi$ (dxz , dyz) metal-based orbitals are high

in energy and there is little effect on the π to π^* energy gap in the regular metalloporphyrins electronic spectra. To some extent, this explains the discrete red shift in the spectra.

The electronic transitions of the porphyrins reported in Tables 1 and 2, indicate that TPPNHAc and TPPNH₂ porphyrins follow Gouterman's four orbital model and there are π - π^* transitions between HOMO-1 and LUMO or LUMO+1. These outcomes match well with other reports, which explain results by referring to transitions between lower occupied, and higher unoccupied molecular orbitals, as well as those from Gouterman's model.^[25–27] The transition follows the same trend as the related porphyrins without Zn. Further experiments with Zn-metalloporphyrins are needed to verify these theoretical predictions.

The HOMO-LUMO gap

As previously indicated in the introduction, useful materials for the design of solar cells must absorb most of the radiation from the solar light in the near-IR and visible regions. For the absorption of light, the value of the HOMO-LUMO gap is crucial. Given that the maximum in the solar radiation energy spectrum corresponds to 2 eV, it is desirable to have an energy gap (HOMO-LUMO) approximating this value. To analyze the possible efficiency of TPPNH₂ and TPPNHAc porphyrins, and the corresponding Zn-metalloporphyrins considering the HOMO-LUMO energy gap, in Figures 2 and 3 we pre-

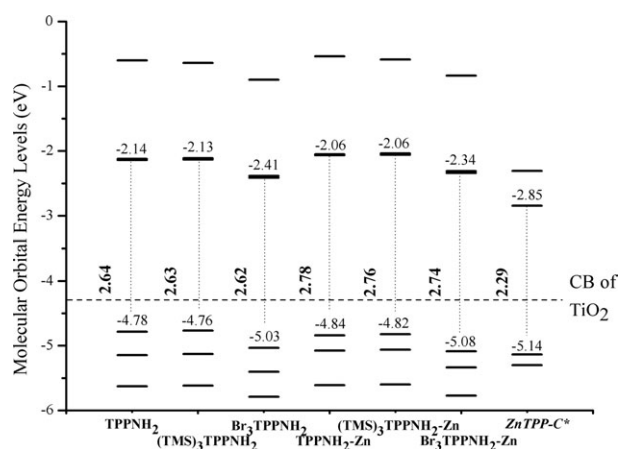


Figure 2. Molecular orbital energy diagram for TPPNH₂ porphyrins. ZnTPP-C was reported in Ref. [17]. CB is the conduction band of titanium oxide.

sented these values and in Tables 3 and 4 we included the molecular orbital picture of the HOMO and the LUMO. For comparison, other values for ZnTPP-C porphyrin that were previously reported are also included in Figures 2 and 3. For TPPNH₂ and TPPNHAc porphyrins bearing different substituents, the HOMO-LUMO energy gap is similar (2.64–2.66 eV), whereas in the case of Zn-metalloporphyrins the HOMO-LUMO energy gap is larger in all cases (2.74–2.80 eV). Comparisons with other previously described porphyrins^[17] are also important and for such comparison it is necessary that the results to have been acquired with the same theoretical approach. In

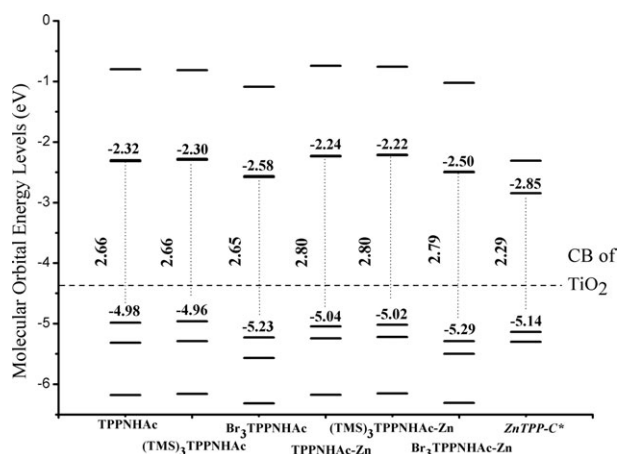


Figure 3. Molecular orbital energy diagram for TPPNHAc porphyrins. ZnTPP-C was reported in Ref. [17]. CB is the conduction band of titanium oxide.

this case, all the results were obtained within the B3LYP approximation. Results illustrated in Figures 2 and 3 indicate that the HOMO–LUMO gaps of all the molecules considered in this study vary from 2.62 ($\text{Br}_3\text{TPPNH}_2$) to 2.80 eV [TPPNHAc-Zn and $(\text{TMS})_3\text{TPPNHAc-Zn}$]. These values are higher by at least 0.33 eV with respect to the ZnTPP-C porphyrins (2.29 eV) previously reported.^[17] However, all values are near 2.0 eV and these types of porphyrins should therefore represent promising materials for solar cell design. Besides, the LUMO values are also important for the efficiency of solar cells, and it is necessary that the LUMO should be situated close to the conduction band of titanium oxide, to increase charge transfer behavior. As presented in Figures 3 and 4, the LUMO of $\text{Br}_3\text{-TPPNH}_2$ and $\text{Br}_3\text{-TPPNHAc}$ porphyrins are closer to the conduction band of titanium oxide than the other porphyrins included in

this study, and they are similar to that previously reported for other molecules (2.41–2.58 vs. 2.85 eV). Consequently, the presence of Br may favor the charge transfer process.

According to Figures 2 and 3, it is evident that Zn increases the HOMO–LUMO gap. For metallated porphyrins, the LUMO are higher in energy and the HOMO are lower in energy. Consequently, the energy difference between the LUMO and the conduction band of titanium oxide is larger, and the HOMO–LUMO energy gap is also higher than that predicted for porphyrins without metal. Apparently the presence of Zn in TPPNH₂ and TPPNHAc porphyrins does not represent an advantage in terms of requirements for solar cell design.

Tables 3 and 4 indicate that the identity of the HOMO and LUMO molecular orbitals are very similar and do not depend on the substituents. In the case of Zn-metalloporphyrins, the $d\pi$ (dxz , dyz) metal-based orbitals correspond to the HOMO orbitals that are lower in energy than the HOMO of the analogous porphyrins. The LUMO orbitals of the metallated porphyrins are higher in energy, but they are similar to the LUMO orbitals of TPPNH₂ and TPPNHAc porphyrins. Consequently, the metal affects the π to π^* energy gap in the electronic spectra, conforming with that expected for regular metalloporphyrins. Overall, the most important difference corresponds to TPPNH₂ and TPPNHAc bearing Br groups. The presence of this substituent produces greater negative values for the molecular orbital energies in all cases, corresponding to the electronegativity of this atom, but the molecular orbital diagram is similar.

Electron-donor acceptor properties

The electron donor–acceptor electronegativities are important in order to determine the electron transfer capability of these molecules. In previous reports^[38,39] the electron donor–acceptor properties were considered simultaneously using a

Table 3. Molecular orbital picture of HOMO and LUMO of TPPNH₂ porphyrins. [Color table can be viewed in the online issue, which is available at [wileyonlinelibrary.com](http://www.intelibrary.com).]

TPPNH ₂	$(\text{TMS})_3\text{TPPNH}_2$	$\text{Br}_3\text{TPPNH}_2$
–2.14 (LUMO)	–2.13 (LUMO)	–2.41 (LUMO)
–4.78 (HOMO)	–4.76 (HOMO)	–5.03 (HOMO)
TPPNH ₂ -Zn	$(\text{TMS})_3\text{TPPNH}_2\text{-Zn}$	$\text{Br}_3\text{TPPNH}_2\text{-Zn}$
–2.06 (LUMO)	–2.06 (LUMO)	–2.34 (LUMO)
–4.84 (HOMO)	–4.82 (HOMO)	–5.08 (HOMO)

The corresponding energy values are given in electron volt.

Table 4. Molecular orbital picture of HOMO and LUMO for TPPNHAc porphyrins. [Color table can be viewed in the online issue, which is available at wileyonlinelibrary.com.]

TPPNHAc		(TMS) ₃ TPPNHAc		Br ₃ TPPNHAc	
-2.32 (LUMO)		-2.30 (LUMO)		-2.58 (LUMO)	
-4.98 (HOMO)		-4.96 (HOMO)		-5.23 (HOMO)	
TPPNHAc-Zn		(TMS) ₃ TPPNHAc-Zn		Br ₃ TPPNHAc-Zn	
-2.24 (LUMO)		-2.22 (LUMO)		-2.50 (LUMO)	
-5.04 (HOMO)		-5.02 (HOMO)		-5.29 (HOMO)	

The corresponding energy values are given in electron volt.

donor–acceptor map (DAM), a novel 2D classification. There, the authors used the DAM to identify the capability as antioxidants or antireductants of several substances such as carotenoids. The DAM is a useful tool for qualitative comparison since any substance can be classified in terms of its electron donating–accepting capability. For the purpose of this investigation, a modified DAM is used. In this case, the electron donor–acceptor electronegativities are used to construct the DAM. The modified DAM shown in Figure 4 is a useful tool for the classification as electron donor–acceptors of the molecules reported in this investigation. There are two regions in the DAM, namely: (1) the good electron acceptor zone where the substance is a bad electron donor (χ^- large) and a good electron acceptor (χ^+ large); (2) the good electron donor zone where the substance is a good electron donor (χ^- small) and

a bad electron acceptor (χ^+ small). The electrons will transfer from the good donor to the good acceptor moiety.

As can be seen in Figure 5, the presence of Br increases χ^- and χ^+ . This means that porphyrins become worse electron

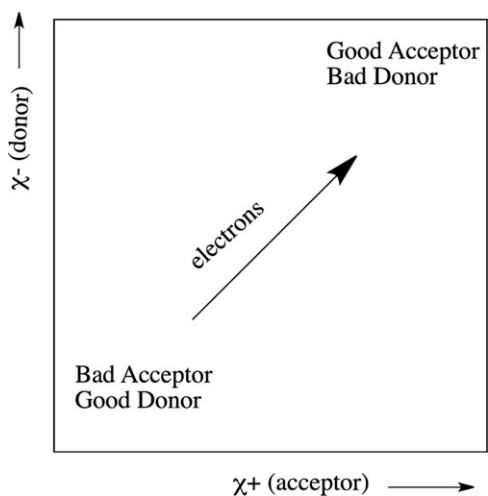


Figure 4. Donor–acceptor map.

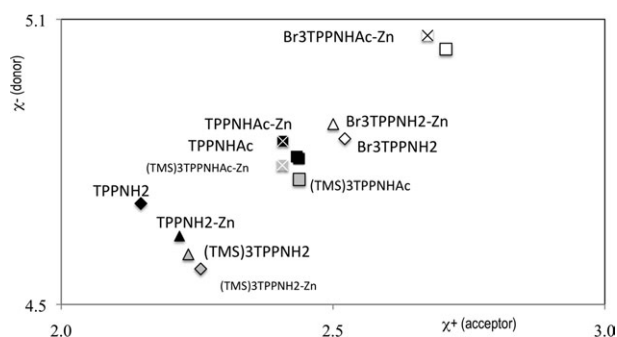


Figure 5. DAM for the molecules under study. χ^- and χ^+ are reported in electron volt.

donors and better electron acceptors due to the presence of Br. This is a logical finding since Br is an electronegative atom. The metal effect is not noticeable in the case of partial electron donor–acceptor properties. Although porphyrins can act either as donor or acceptor units, depending on whether they are metallated or not; in most cases these chromophores behave as acceptors in molecular antennae and collect the energy emitted from other donor units. For this reason, it is desirable to increase the electron acceptor properties. We can augment this acceptor characteristic by introducing electron-withdrawing groups into their structure, when the acceptor effect of metallation is not strong enough. This is the case with the Br atom that has more effect on electron donor–acceptor properties than metallation. In summary, metallation

with Zn does not represent an advantage over no-metallated porphyrins in terms of electron donor–acceptor properties, but the presence of Br increment the electron acceptor capability.

Conclusions

● TPPNH₂ and TPPNHAc porphyrins have asymmetric substituted rings and present strongly mixed configurations. All the electronic transitions follow Gouterman's four orbital model, the electronic transitions are found in HOMO–1 to LUMO or LUMO+1.

● The bands of TPPNH₂ and TPPNHAc bearing acceptor groups, such as Br are red-shifted with respect to the non substituted porphyrins. This is desirable quality in the case of dye-sensitized solar cells. Zn-metalloporphyrins bands are slightly red shifted, due to the presence of the metal in all cases. The transition follows the same trend as the related porphyrins without Zn. Further experiments with Zn-metalloporphyrins are needed to verify these theoretical predictions.

● The HOMO–LUMO gaps of TPPNH₂ and TPPNHAc porphyrins are close to 2.0 eV and consequently, these compounds should be good materials for solar cell design. Moreover, the absorption of light would be facilitated in the case of systems with smaller HOMO–LUMO gaps and this might be an advantage for TPPNH₂ and TPPNHAc porphyrins, when compared to others.


● The electron donor–acceptor properties of porphyrins and metallated porphyrins of this investigation are similar. The presence of Br, an acceptor group, increases the electron acceptor properties, something that could be useful for future applications.

Acknowledgments

CC is grateful for doctoral scholarship from CONACYT–México (number 226754). The authors are grateful to PAPIIT (Project IN105610) and CONACYT (Project 128788). The work was carried out, using a KanBalam supercomputer, provided by DGTIC, UNAM. The authors would like to acknowledge both Oralia L. Jiménez A and María Teresa Vazquez for Technical support.

Keywords: solar cells · TD-DFT · absorption · electro-negativity · synthesis of porphyrins

How to cite this article: C. Caicedo, A. Martínez, E. Rivera, *Int. J. Quantum Chem.* **2013**, *113*, 1376–1383. DOI: 10.1002/qua.24316

 Additional Supporting Information may be found in the online version of this article.

- [1] R. J. M. K. Gebbink, B. M. J. M. Suijkerbuijk, *Angew. Chem. Int. Ed. Engl.* **2008**, *47*, 7396.
- [2] M. O. Senge, M. Fazekas, E. G. A. Notaras, W. Blau, J. Zawadzka, M. O. B. Locos, E. M. N. Mhuircheartaigh, *Adv. Mater.* **2007**, *19*, 2737.
- [3] M. Pawlicki, H. A. Collins, R. G. Denning, H. L. Anderson, *Angew. Chem. Int. Ed. Engl.* **2009**, *48*, 3244.
- [4] H. L. Anderson, *Chem. Commun.* **1999**, *23*, 2323.
- [5] J. Li, L. Yuliang, *J. Porph. Phthal.* **2007**, *11*, 299.
- [6] L. Petit, A. Quartarotolo, A. Adamo, N. Russo, *J. Phys. Chem. B.* **2006**, *110*, 2398.
- [7] M. R. Wasielewski, *Chem. Rev.* **1992**, *92*, 435.
- [8] (a) R. W. Wagner, J. S. Lindsey, J. Seth, V. Palaniappan, D. F. Bocian, *J. Am. Chem. Soc.* **1996**, *118*, 3996; (b) A. Ambrosio, R. W. Wagner, P. D. Rao, J. A. Riggs, P. Hascoat, J. R. Diers, J. Seth, R. K. Lammi, D. F. Bocian, D. Holten, J. S. Lindsey, *Chem. Mater.* **2001**, *13*, 1023.
- [9] P. A. Liddell, G. Kodis, A. L. Moore, T. A. Moore, D. Gust, *J. Am. Chem. Soc.* **2002**, *124*, 7668.
- [10] X. Camps, E. Dietel, A. Hirsch, S. Pyo, L. Echegoyen, S. Hackbarth, B. Röder, *Chem. Eur. J.* **1999**, *5*, 2362.
- [11] (a) J. Brettar, J.-P. Gisselbrecht, M. Gross, N. Solladié, *Chem. Commun.* **2001**, *8*, 733; (b) L. Flamigni, A. M. Talarico, B. Ventura, R. Rein, N. Solladié, *Chem. Eur. J.* **2006**, *12*, 701.
- [12] (a) G. Knör, *Inorg. Chem. Commun.* **2001**, *4*, 160; (b) N. Sheng, J. Sun, Y. Bian, J. Jiang, D. Xu, *J. Porph. Phthal.* **2009**, *13*, 275; (c) M. Zhu, Y. Lu, Y. Du, J. Li, X. Wang, P. Yang, *Int. J. Hydrogen Energy.* **2011**, *36*, 4298.
- [13] T. D. M. Bell, S. V. Bhosale, K. P. Ghiggino, S. J. Langford, C. P. Woodard, *Aust. J. Chem.* **2009**, *62*, 692.
- [14] S. V. Natarajan, S. Ambigapathy, N. Hitoshi, M. Hiroshi, K. Yoshiyuki, *Int. J. Quantum Chem.* **2011**, *111*, 2340.
- [15] N. Katsunori, K. Kei, O. Atsuhiko, U. Masanobu, K. Nagao *J. Inorg. Biochem.* **2008**, *102*, 466.
- [16] Y.-H. Zhang, L.-H. Zhao, W.-J. Ruan, Y. Xu, *Spectrochim. Acta Part A.* **2011**, *79*, 1449.
- [17] M. P. Balanay, D. H. Kim, *Phys. Chem. Chem. Phys.* **2008**, *10*, 5121.
- [18] O. Cramariuc, T. I. Hukka, T. T. Rantala, *J. Phys. Chem. A.* **2004**, *108*, 9435.
- [19] D. S. Corinne, L. B. Jonathan, L. S. Amy, W. Birgit, L. Nicolai, *Inorg. Chem. Acta.* **2012**, *380*, 148.
- [20] L. Xia, K. L. Y. Edwin, V. Suresh, P. S. Ronald, *Phys. Chem. Chem. Phys.* **2006**, *8*, 1298.
- [21] L.-F. Wang, X.-W. Meng, F.-Q. Tang, *J. Mol. Struct. (THEOCHEM)* **2010**, *956*, 26.
- [22] (a) M. Ruimin, P. Guo, H. Cui, X. Zhang, K. M. Nazeeruddin, M. Grätzel, *J. Phys. Chem. A.* **2009**, *113*, 10119; (b) M. Ruimin, P. Guo, L. Yang, L. Guo, Q. Zeng, G. Liu, X. Zhang, *J. Mol. Struct. (THEOCHEM)* **2010**, *942*, 131.
- [23] Y. Zhu, S. Zhou, Y. Kan, Z. Su, *Int. J. Quantum Chem.* **2007**, *107*, 1614.
- [24] M. E. Casida, *J. Mol. Struct. (THEOCHEM)* **2009**, *914*, 3.
- [25] M. Gouterman, *J. Mol. Spectrosc.* **1961**, *6*, 138.
- [26] M. Gouterman, G. H. Wagniere, *J. Mol. Spectrosc.* **1963**, *11*, 108.
- [27] M. Gouterman, *J. Chem. Phys.* **1959**, *30*, 1139.
- [28] D. Jacquemin, E. A. Perpète, I. Ciodini, C. Adamo, *J. Chem. Theor. Comput.* **2010**, *6*, 1532.
- [29] W. Kohn, A. D. Becke, R. G. Parr, *J. Phys. Chem.* **1996**, *100*, 12974.
- [30] (a) P. Hohenberg, W. Kohn, *Phys. Rev.* **1964**, *136*, B864; (b) W. Kohn, L. Sham, *J. Phys. Rev.* **1965**, *140*, A1133.
- [31] M. J. Frisch, G. W. Trucks, H. B. Schlegel, G. E. Scuseria, M. A. Robb, J. R. Cheeseman, G. Scalmani, V. Barone, B. Mennucci, G. A. Petersson, H. Nakatsuji, M. Caricato, X. Li, H. P. Hratchian, A. F. Izmaylov, J. Bloino, G. Zheng, J. L. Sonnenberg, M. Hada, M. Ehara, K. Toyota, R. Fukuda, J. Hasegawa, M. Ishida, T. Nakajima, Y. Honda, O. Kitao, H. Nakai, T. Vreven, J. A. Montgomery, Jr., J. E. Peralta, F. Ogliaro, M. Bearpark, J. J. Heyd, E. Brothers, K. N. Kudin, V. N. Staroverov, R. Kobayashi, J. Normand, K. Raghavachari, A. Rendell, V. G. Zakrzewski, G. A. Voth, P. Salvador, J. J. Dannenberg, S. Dapprich, A. D. Daniels, Á. Farkas, J. B. Foresman, J. V. Ortiz, J. Cioslowski, D. J. Fox, Gaussian 09 Revision A.1; Gaussian Inc.: Wallingford CT, **2009**.
- [32] (a) A. D. Becke, *Phys. Rev. A.* **1988**, *38*, 3098; (b) B. Mielich, A. Savin, H. Stoll, H. Peuss, *Chem. Phys. Lett.* **1989**, *157*, 200; (c) C. Lee, W. Yang, R. G. Parr, *Phys. Rev. B.* **1988**, *37*, 785.
- [33] (a) G. A. Petersson, A. Bennett, T. G. Tensfeldt, M. A. Al-Laham, W. A. Shirley, J. Mantzaris, *J. Chem. Phys.* **1988**, *89*, 2193; (b) G. A. Petersson, M. A. Al-Laham, *J. Chem. Phys.* **1991**, *94*, 6081.
- [34] M. T. Cancès, B. Mennucci, J. Tomasi, *J. Chem. Phys.* **1997**, *107*, 3032.
- [35] B. Mennucci, J. Tomasi, *J. Chem. Phys.* **1997**, *106*, 5151.

- [36] J. L. Gázquez, A. Cedillo, A. Vela, *J. Phys. Chem. A* **2007**, *111*, 1966; (b) J. L. Gázquez, *J. Mex. Chem. Soc.* **2008**, *52*, 3; (c) J. Z. Ramírez-Ramírez, R. Vargas, J. Garza, J. L. Gázquez, *J. Phys. Chem. A* **2010**, *114*, 7945.
- [37] (a) M. Avelar, A. Martínez, *J. Mex. Chem. Soc. (in press)*; (b) F. J. Tenorio, R. Sato-Berrú, J. M. Saniger, A. Martínez, *Int. J. Quantum Chem.* DOI: 10.1002/qua.24153.
- [38] L. H. Skibsted, *J. Agric Food Chem* **2012**, *60*, 2409.
- [39] (a) A. Martínez, M. A. Rodríguez-Gironés, A. Barbosa, M. Costas, *J. Phys. Chem. A* **2008**, *112*, 9037; (b) A. Martínez, *J. Phys. Chem. B* **2009**, *113*, 4915.

Received: 22 June 2012
 Revised: 24 July 2012
 Accepted: 25 July 2012
 Published online on 13 August 2012